Photoionization of atomic beryllium from the ground state

Dae-Soung Kim* and Swaraj S. Tayal
Department of Physics, Clark Atlanta University, Atlanta, Georgia 30314

Hsiao-Ling Zhou and Steven T. Manson
Department of Physics and Astronomy, Georgia State University, Atlanta, Georgia 30303
(Received 9 November 1999; published 3 May 2000)

Photoionization of the ground $1s^2 2s^2\ ^1S$ state of atomic beryllium is studied in the energy region between the $Be^+(2s)$ and $Be^+(3d)$ thresholds using a noniterative variational *R*-matrix method combined with multichannel quantum-defect theory at the *R*-matrix surface. The autoionizing Rydberg series of resonances converging to the Be^+ ($2p$, $3s$, $3p$, and $3d$) thresholds are identified and effective quantum numbers assigned. Also calculated are the photoelectron angular distribution asymmetry parameters β for the processes leaving the ion in the Be^+ ($1s^2 np$, $n=2,3$) states. The present photoionization cross sections extend earlier work and are in good agreement with previous calculations and experiments. There is excellent agreement between length and velocity gauges in our calculation.

PACS number(s): 32.80.Fb

I. INTRODUCTION

There has been great theoretical and experimental interest in photoabsorption studies of atoms and ions with two valence electrons. Because of the relative simplicity of these atomic systems, it is possible to understand the electron correlation effects in some detail. After helium, atomic Be($1s^2 2s^2\ ^1S$) is the next simplest atomic system with two valence electrons outside the $1s^2$ core. In addition, it is of importance astrophysically owing to its abundance. The first theoretical calculation for photoionization of the ground state of atomic Be was performed by Altick [1]. He found that the near-threshold photoionization cross section is dominated by the $2pns$ and $2pnd$ autoionization series. Mehlman-Balloffet and Esteva [2,3] measured the photoionization spectrum of the Be atom. In this experiment some absorption lines were observed that were not due to the neutral atom and it was difficult to see the $2pnd$ resonances. Dubau and Wells [4] calculated photoionization cross sections using quantum-defect theory and showed that there is satisfactory agreement between the shapes of the theoretical and experimental results. Greene [5] used a hyperspherical coordinate approach and O'Mahony and Greene [6] used a noniterative eigenchannel *R*-matrix method to study the doubly excited states of Be. Radojevic and Johnson [7] developed a multiconfiguration Tamm-Dancoff (MCTD) method to study photoexcitation of atoms in cases where the simultaneous excitation of two atomic electrons is important, and calculated cross sections for Be. Moccia and Spizzo [8] obtained the photoionization cross sections of the ground state of Be in the energy region below the $Be^+(2p)$ threshold using variational wave functions. Tully *et al.* [9] calculated photoionization cross sections of the beryllium sequence using Opacity Project (OP) *R*-matrix codes [10]. Chi *et al.* [11] used a multiconfiguration relativistic random-phase approximation to investigate the autoionizing levels of Be near its first ionization threshold. Calculations using a *B*-spline-based configuration-interaction procedure were performed by Chang, Tang, and Zhu [12]. Zhou and Lin [13] calculated photoionization cross sections of the ground state of the Be atom by the use of a hyperspherical close-coupling (HSCC) method and employed a model potential to describe the screening of frozen closed-shell electrons. They extended the energy range up to the $Be^+(3s)$ threshold and calculated total as well as partial cross sections for the photoionization of the ground state in length and acceleration approximations. They did not calculate velocity results because of difficulties in the HSCC method.

Most of the earlier studies focused on the photoionization of Be in the energy region between the $Be^+(2s)$ and $Be^+(3s)$ thresholds. In order to provide a more complete picture, in the present work we report total and partial cross sections for the photoionization of the ground state $1s^2 2s^2\ ^1S$ for photon energies from the $Be^+(2s)$ threshold to the $Be^+(3d)$ threshold. The calculations are performed using the variational *R*-matrix method [14], which is a reformulation of the noniterative eigenchannel *R*-matrix method. We extended this method to get partial cross sections for the various channels. There are six channels $2s\epsilon p$, $2p\epsilon s$, $2p\epsilon d$, $3s\epsilon p$, $3p\epsilon s$, and $3p\epsilon d$ below the $Be^+(3d)$ threshold that are allowed by dipole selection rules in the photoionization of the Be $1s^2 2s^2\ ^1S$ state. We also present our results for the photoelectron angular distribution asymmetry parameter β for the $Be^+(1s^2 np\ ^2P)$, $n=2,3$, channels; the other final states of Be^+ are *S* states which lead to a constant $\beta=2$.

With a brief description of the theoretical method used for the present calculation in the next section, the results are presented and discussed in Sec. III.

II. CALCULATIONAL DESCRIPTION

Neglecting relativistic effects, the Hamiltonian of the two valence electrons of the Be atom outside the closed-shell $1s^2$ core can be written (in atomic units) as

*Present address: Department of Internet Business, Song Ho College, Heongsung Gun, Kangwon-Do 225-800, Republic of Korea.

TABLE I. Values of parameters for the effective potential $U_l(r)$.

Atom	l	α_1^l	α_2^l	α_3^l	α_{cp}	r_c
Be	0–4	5.59790	7.40190	6.16890	0.05182	0.4

$$H=H(r_1)+H(r_2)+\frac{1}{r_{12}}, \tag{2.1}$$

where $H(r)=-\frac{1}{2}\nabla^2+U(r)$ represents the one-electron Hamiltonian. The wave functions of the outer two electrons are expressed in terms of independent-particle wave functions given by

$$\left(-\frac{1}{2}\frac{d^2}{dr^2}+\frac{l(l+1)}{2r^2}+U(r)-E_{nl}\right)\phi_{nl}(r)=0, \tag{2.2}$$

where $U(r)$ describes the effective potential for the e-Be^{2+} interaction. We have adopted the following form of $U(r)$ [15]:

$$U(r)=-\frac{1}{r}[2+(Z-2)e^{-\alpha_1^l r}+\alpha_2^l e^{-\alpha_3^l r}] - \frac{\alpha_{cp}}{2r^4}(1-e^{-(r/r_c)^3})^2, \tag{2.3}$$

where we have used the calculated values of Johnson *et al.* [16] for α_{cp}. The parameters α_i and r_c are chosen to optimize agreement between the calculated and experimental energy levels of the ground and valence excited states of Be. The values of the parameters for the effective potential $U(r)$ in Eq. (2.3) are given in Table I. Using Eq. (2.2), a basis set of the lowest 20 orbitals for each $l\leqslant 3$, ϕ_{nl}^c, which vanish at the R-matrix boundary, $r=r_0=14$ a.u., is obtained. In addition, the lowest two positive energy solutions for each l are generated, ϕ_{nl}^o, whose derivatives vanish at the boundary, and they are added to the basis set. It is noted that all closed orbitals are orthogonal to each other, and good convergence is achieved in the present calculation with an accuracy of 10^{-8} or better. A particular LS coupled two-electron orbital is expressed by

$$y_{n_1l_1,n_2l_2}=\frac{1}{\sqrt{2}}[\phi_{n_1l_1}(r_1)\phi_{n_2l_2}(r_2)Y_{l_1l_2LM}(\Omega_1,\Omega_2) + q\phi_{n_2l_2}(r_1)\phi_{n_1l_1}(r_2)Y_{l_2l_1LM}(\Omega_1,\Omega_2)], \tag{2.4}$$

where $q=(-1)^{l_1+l_2-L+S}$. The matrix elements of the one-electron Hamiltonian $H(r)$ are easily calculated since the basis functions (2.4) are the eigenfunctions of $H(r_1)+H(r_2)$. On the other hand, the evaluation of matrix elements for $1/r_{12}$ is more complicated, but they need to be evaluated only once since our basis set is energy independent.

The noniterative formulation of the variational R-matrix method used in the present study has been discussed in detail by Robicheaux [14]. We summarize it only briefly. To begin with, the essential difference between the method used here and the traditional R-matrix calculation [10] is that, in the present treatment, the effects of inner shells ($1s^2$ in this case) are represented by a central potential, adjusted as described. The R-matrix eigenchannel functions ψ_β are the eigenstates of the Hamiltonian (2.1) at any desired energy E whose negative logarithmic derivatives b_β are constant over the surface S enclosing the reaction volume [17]. Then, b_β is an eigenvalue of a generalized linear eigensystem

$$\Gamma c=b_\beta \Lambda c, \tag{2.5}$$

where

$$\Gamma_{ij}=2\int_V y_i(E-H)y_i dv-\int_s y_i\frac{\partial y_j}{\partial n}ds, \qquad \Lambda_{i,j}=\int_s y_i y_j ds. \tag{2.6}$$

The variational wave function $\psi_\beta=\Sigma_i c_{i\beta}y_i$ related to an eigenvalue b_β can be expressed as

$$\langle\phi_i|\psi_\beta\rangle=f_i(r)I_{i\beta}-g_i(r)J_{i\beta}, \quad r\geqslant r_0, \tag{2.7}$$

and its normal derivative by

$$\left\langle\phi_i\left|\frac{\partial\psi_\beta}{\partial r}\right\rangle\right.=\frac{\partial}{\partial r}f_i(r)I_{i\beta}-\frac{\partial}{\partial r}g_i(r)J_{i\beta}, \quad r=r_0, \tag{2.8}$$

where the ϕ_i represent atomic core states, and $f_i(r)$ and $g_i(r)$ are the regular and irregular Coulomb wave functions evaluated at the photoelectron energy $E_i=\omega-\epsilon_i$ (in channel i associated with photon energy ω). The $N\times N$ reaction matrix and its diagonalization is given by

$$K=JI^{-1} \tag{2.9}$$

and its diagonalization is performed by

$$K_{ij}=\sum_\alpha U_{i\alpha}\tan(\pi\mu_\alpha)(U^T)_{\alpha j}, \tag{2.10}$$

where $U_{i\alpha}$ and μ_α are the eigenvector elements and eigenquantum defects. The energy-normalized eigenstates ψ_α in each channel i can be represented by the linear combinations of the unnormalized R-matrix eigenstates ψ_β [6],

$$\psi_\alpha=\sum_{\beta,i}\psi_\beta(I^{-1})_{\beta i}U_{i\alpha}\cos(\pi\mu_\alpha). \tag{2.11}$$

These variational wave functions are connected to the reduced dipole matrix elements in the length form as

$$d_\alpha(L)=\langle\psi_\alpha\|\vec{r}_1+\vec{r}_2\|\psi_0\rangle \tag{2.12}$$

and in the velocity form as

TABLE II. Ionization thresholds (in eV) relative to the ground state of atomic Be.

State	Theory	Experiment [24]
$1s^2 2s\ ^2S$	9.2959	9.320
$1s^2 2p\ ^2P$	13.2543	13.277
$1s^2 3s\ ^2S$	20.2305	20.257
$1s^2 3p\ ^2P$	21.2688	21.281
$1s^2 3d\ ^2D$	21.4569	21.474

$$d_\alpha(V)=\frac{1}{\omega}\langle\psi_\alpha\|\vec{\nabla}_1+\vec{\nabla}_2\|\psi_0\rangle, \tag{2.13}$$

where ψ_0 represents the ground state wave function. The deviation between the length and velocity results gives a measure of the inaccuracy of the variational wave functions employed.

A. Cross section

In order to calculate partial and total photoionization cross sections, we need to find a new set of solutions $\psi_i(\epsilon)$ with $i=1,\ldots,N_o$ from ψ_α which should remain well behaved at $r\to\infty$. The $N_o\times N_o$ open-channel reaction matrix is written as [18]

$$K^{oo}_{phys}=K^{oo}-K^{oc}(K^{cc}+\tan\pi n^*)^{-1}K^{co}, \tag{2.14}$$

where the diagonal matrix of effective quantum numbers in the closed channels is given by

$$n^*=\frac{1}{\sqrt{2(E_t-\omega)}}, \tag{2.15}$$

where E_t represents the target state. The diagonalization of K^{oo}_{phys} gives eigenvalues λ_i. The eigenphase in each channel is then defined as

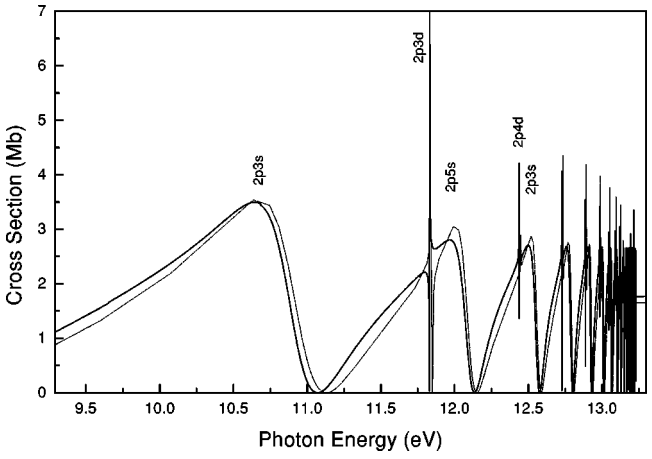

FIG. 1. Total photoionization cross section for the ground state of Be below the $Be^+(2p)$ threshold as a function of photon energy. Solid curve, present calculation; dotted curve, OP result [9].

TABLE III. Resonance positions (E_r in eV), effective quantum numbers (n^*), and widths (Γ in eV) of autoionizing levels converging to the $Be^+(2p)$ threshold.

	Present result			Other results		
State	E_r	n^*	Γ	E_r [2]	n^* [2]	E_r [1]
$2p3s$	10.9103	2.4093	1.4206	10.7068	2.30	10.77
$2p4s$	12.0918	3.4211	0.4948	11.9678	3.22	12.07
$2p5s$	12.5579	4.4202	0.2237	12.5339	4.26	12.60
$2p6s$	12.7911	5.4196	0.1196	12.7820	5.22	
$2p7s$	12.9239	6.4174	0.0714	12.9219	6.15	
$2p8s$	13.0070	7.4174	0.0460	13.0100	7.08	
$2p9s$	13.0623	8.4170	0.0314			
$2p10s$	13.1009	9.4163	0.0224			
$2p11s$	13.1289	10.4151	0.0165			
$2p12s$	13.1498	11.4124	0.0125			
$2p13s$	13.1660	12.4104	0.0097			
$2p14s$	13.1786	13.4093	0.0077			
$2p15s$	13.1888	14.4076	0.0062			
$2p3d$	11.8310	3.0918	0.0010	11.8623	3.10	11.86
$2p4d$	12.4374	4.0812	0.0010	12.4658	4.08	12.49
$2p5d$	12.7272	5.0807	0.0009	12.7570	5.09	12.47
$2p6d$	12.8863	6.0806	0.0007	12.9192	6.13	
$2p7d$	12.9829	7.0804	0.0002			
$2p8d$	13.0458	8.0780	0.0001			
$2p9d$	13.0893	9.0751				
$2p10d$	13.1201	10.0672				
$2p11d$	13.1431	11.0650				
$2p12d$	13.1608	12.0635				
$2p13d$	13.1745	13.0594				
$2p14d$	13.1853	14.0421				
$2p15d$	13.1941	15.0356				

$$\delta_i=\tan^{-1}\lambda_i, \quad i=1,\ldots,N_o. \tag{2.16}$$

The eigenphase sum δ is the sum over δ_i. The associated dipole matrix element is given by [20]

$$d^o_{phys}=d^o_\alpha-d^c_\alpha(K^{cc}+\tan\pi n^*)^{-1}K^{co}, \tag{2.17}$$

where d^o_α and d^c_α are the dipole matrix elements, Eq. (2.12) or (2.13), corresponding to open and closed channels, respectively, essentially the same as Eq. (2.58) of Ref. [20]. The partial photoionization cross section is given by

$$\sigma_i=\frac{4\pi^2}{3(137)}\omega|d_i^{(-)}|^2 \tag{2.18}$$

in atomic units, where

$$d_i^{(-)}=\frac{d^o_{phys}}{1+iK^{oo}_{phys}} \tag{2.19}$$

is the outgoing dipole matrix element. Finally, the total photoionization cross section is given by

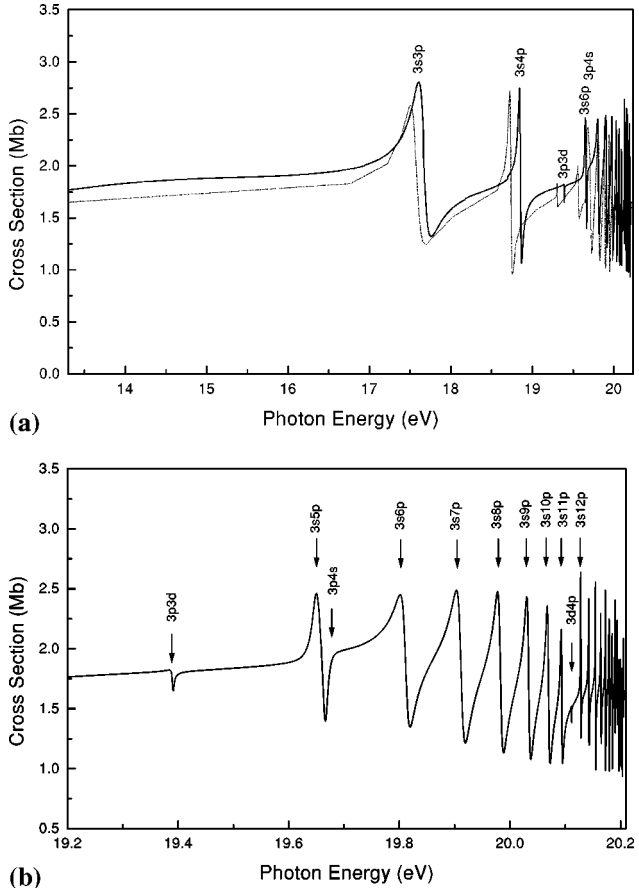

FIG. 2. Total photoionization cross section for the ground state of Be between the $Be^+(2p)$ and $Be^+(3s)$ thresholds: (a) cross section as a function of photon energy in eV; (b) detail of cross section in the resonance region. Solid curve, present calculation; dotted curve, OP result [9].

$$\sigma = \frac{4\pi^2}{3(317)}\omega \sum_i |d_i^{(-)} d_i^{(-)\dagger}|. \tag{2.20}$$

B. Photoelectron angular distribution

The differential cross section for photoionization in the dipole approximation is given by [19]

$$\frac{d\sigma_i}{d\Omega} = \frac{\sigma_i}{4\pi}[1 + \beta_i P_2(\cos\theta)], \tag{2.21}$$

where θ is the angle between the photon polarization and photoelectron direction, $P_2(\cos\theta) = (3\cos\theta^2 - 1)/2$, and β_i is the photoelectron angular distribution asymmetry parameter; its detailed formulation is given elsewhere [21]. Using the angular momentum transfer analysis [22], it is found that the photoelectron angular distribution parameter β_{np} for leaving the ion in a $Be^+(np)$ state is given by

$$\beta_{np} = \frac{d_{\epsilon d}^2 + \sqrt{2}(d_{\epsilon s} d_{\epsilon d}^{\dagger} + \text{c.c.})}{d_{\epsilon s}^2 + d_{\epsilon d}^2} \tag{2.22}$$

TABLE IV. Resonance positions (E_r in eV), effective quantum numbers (n^*), and widths (Γ in eV) of the $3snp\ ^1P$ autoionizing levels converging to the $Be^+(3s)$ threshold.

	Present result			Other results	
State	E_r	n^*	Γ	E_r [2]	E_r [3]
$3s3p$	17.6640	2.3025	0.5074	17.6441	17.6844
$3s4p$	18.8548	3.1449	0.0751	18.7970	18.8342
$3s5p$	19.6524	4.8514	0.0512		
$3s6p$	19.8119	5.7011	0.0559	19.8059	19.7965
$3s7p$	19.9117	6.5335	0.0511	19.9141	19.9141
$3s8p$	19.9828	7.4112	0.0348		19.9944
$3s9p$	20.0336	8.3142	0.0231		20.0461
$3s10p$	20.0696	9.1955	0.0155		
$3s11p$	20.0935	9.9671	0.0076		
$3s12p$	20.1278	11.5117	0.0019		
$3s13p$	20.1430	12.4747	0.0022		
$3s14p$	20.1553	13.4523	0.0031		
$3s15p$	20.1651	14.4248	0.0022		

with the dipole matrix elements given by Eq. (2.19) with the superscripts $(-)$ omitted to avoid confusion, and where the subscripts (s,d) refer to the transitions from the initial $1s^2 2s^2\ ^1S$ state to $(1s^2 np\ ^2P)\epsilon s$ and $(1s^2 np\ ^2P)\epsilon d$ states, respectively. The Coulomb phase difference, $\sigma = \sigma_d - \sigma_s$, can be obtained analytically [23]:

$$\sigma = \sigma_d - \sigma_s = -\tan^{-1}\left(\frac{3z}{2(2\epsilon)^{1/2} - z^2(2\epsilon)^{-1/2}}\right), \tag{2.23}$$

where z is the asymptotic charge experienced by the photoelectron ($z=1$ for the Be atom) and ϵ is the photoelectron energy in atomic units.

III. RESULTS AND DISCUSSION

We have calculated total and partial photoionization cross sections from the ground state $1s^2 2s^2\ ^1S$ for photon energies between the $Be^+(2s)$ and $Be^+(3d)$ thresholds in both the length and velocity gauges. There is excellent agreement between the length and velocity results in the entire photon energy region considered in our work, which indicates that our cross sections are likely to be very accurate. We studied the following photoionization processes:

$$\text{Be}(1s^2 2s^2\ ^1S) + \gamma \rightarrow \text{Be}^+(1s^2 ns\ ^2S) + \epsilon p(^1P) \tag{3.1}$$

$$\rightarrow \text{Be}^+(1s^2 np\ ^2P) + \epsilon s(^1P) \tag{3.2}$$

$$\rightarrow \text{Be}^+(1s^2 np\ ^2P) + \epsilon d(^1P), \tag{3.3}$$

for $n = 2,3$, where γ represents the incident photon.

The calculated and experimental energies of the ionization thresholds relative to the ground state $1s^2 2s^2\ ^1S$ are

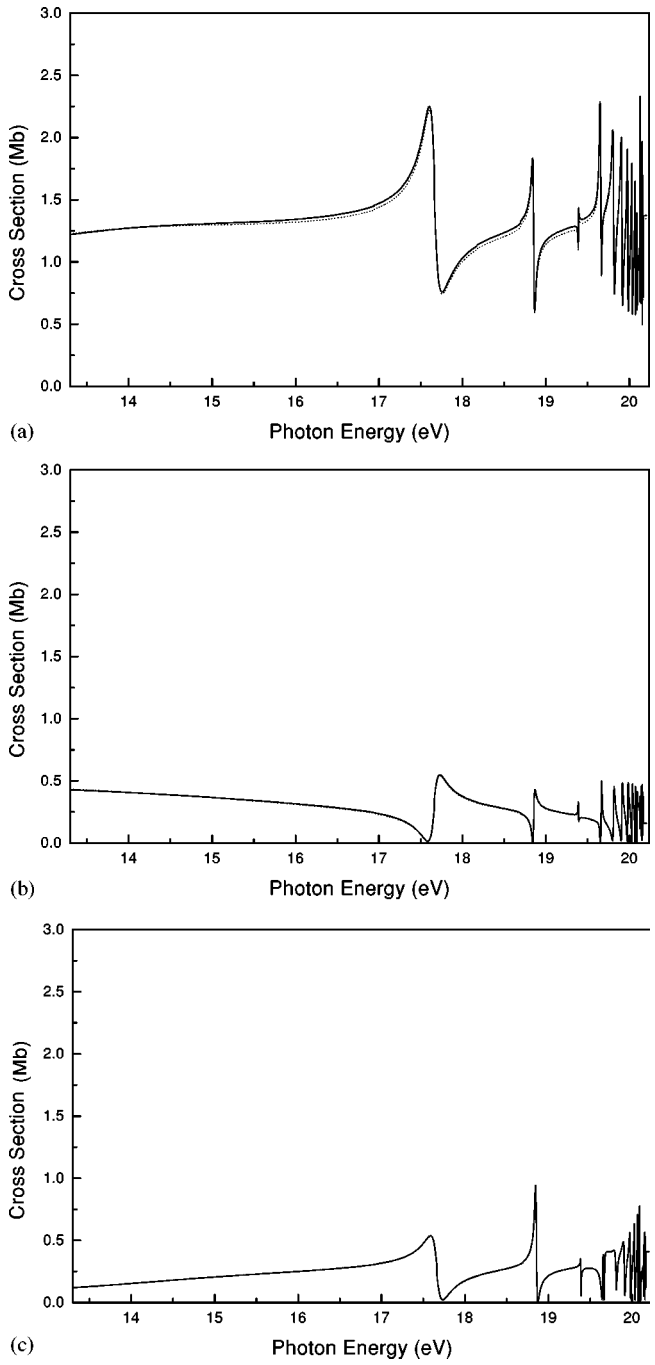

FIG. 3. Partial photoionization cross sections: (a) $\sigma_{2s\epsilon p}$, (b) $\sigma_{2p\epsilon s}$, (c) $\sigma_{2p\epsilon d}$ as a function of photon energy. Solid curve, present length values; dashed curve, present velocity values.

given in Table II. Agreement between our calculated results and the experimental numbers from Ref. [24] is excellent; within 25 meV.

In the energy region below the $Be^+(2p)$ threshold there are two closed channels $2pns$ and $2pnd$ which give rise to two Rydberg series of autoionizing resonances converging to the $Be^+(2p)$ threshold, and one open channel $2p\epsilon s$. The present length values of the photoionization cross section in this energy region are displayed by the solid curve in Fig. 1 along with the earlier calculation of the Opacity Project [9]

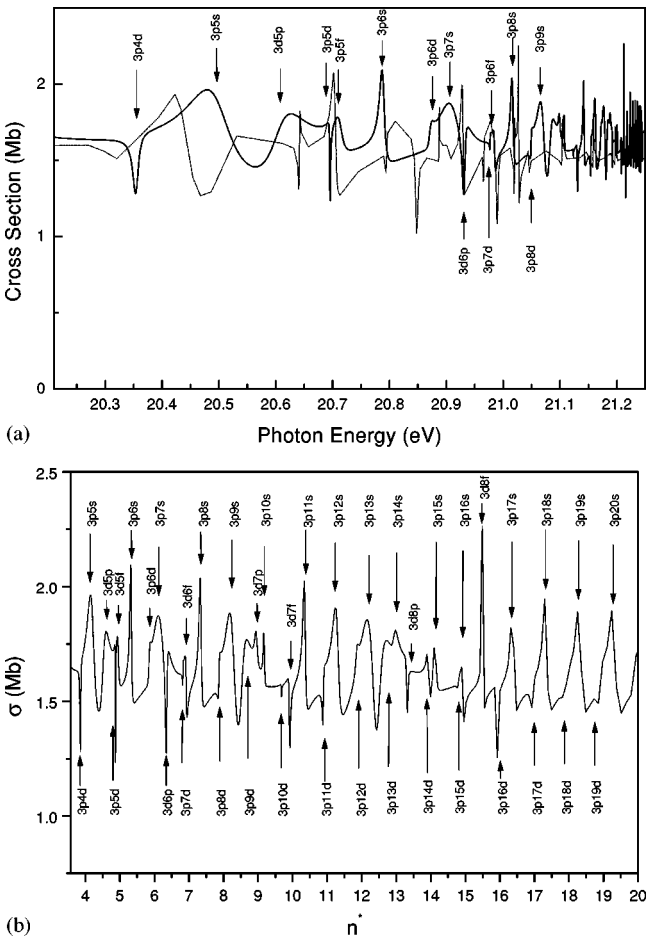

FIG. 4. Total photoionization cross section for the ground state of Be between the $Be^+(3s)$ and $Be^+(3p)$ thresholds: (a) cross section as a function of photon energy in eV; (b) cross section as a function of effective quantum number n^*. Arrows indicate the positions of the autoionizing levels. Solid curve, present calculation; dotted curve, OP result [9].

shown by a dotted curve as a function of photon energy. The two calculations show excellent agreement. Two Rydberg series of doubly excited states, a broad $2pns$ series and a narrow $2pnd$ series, can be clearly identified in Fig. 1.

A resonance position E_r may be defined as the energy at which the eigenphase sum δ has its maximum value of $d\delta/dE$ [25]. The width of the resonance Γ is related to the inverse of the eigenphase gradient and it is equivalent to the time-delay matrix Q [26],

$$\Gamma = 2\left(\frac{d\delta}{dE}\right)^{-1}_{E=Er}. \tag{3.4}$$

Since the $2pnd$ series of resonances are very narrow, they decay slowly. Calculated energies E_r, effective quantum numbers n^*, and widths Γ of the autoionizing levels of the $2pns$ and $2pnd$ series are listed in Table III and are compared with the available data [1,2]. Our results are in agreement with experimental data [2]. O'Mahony and Greene [6] reported total photoionization cross sections of Be from the ground state in the energy region below the $Be^+(2p)$ thresh-

TABLE V. Resonance positions (E_r in eV), effective quantum numbers (n^*), and widths (Γ in eV) of autoionizing levels $3pns$ and $3pnd$ converging to the $Be^+(3p)$ threshold.

State	E_r	n^*	Γ	State	E_r	n^*	Γ
				$3p3d$	19.3919	2.6919	0.0045
$3p4s$	19.6687	2.9160	0.0056	$3p4d$	20.3556	3.8597	0.0056
$3p5s$	20.4990	4.2041	0.2407	$3p5d$	20.6963	4.8749	0.0038
$3p6s$	20.7951	5.3591	0.0060	$3p6d$	20.8729	5.8622	0.0053
$3p7s$	20.9254	6.2945	0.0059	$3p7d$	20.9877	6.9574	0.0054
$3p8s$	21.0163	7.3405	0.0156	$3p8d$	21.0498	7.8815	0.0040
$3p9s$	21.0729	8.3338	0.0056	$3p9d$	21.0816	8.5254	0.0033
$3p10s$	21.1099	9.2535	0.0058	$3p10d$	21.1241	9.6953	0.0050
$3p11s$	21.1420	10.3593	0.0063	$3p11d$	21.1537	10.8732	0.0023
$3p12s$	21.1622	11.2951	0.0111	$3p12d$	21.1717	11.8360	0.0031
$3p13s$	21.1807	12.4243	0.0103	$3p13d$	21.1875	12.9335	0.0057
$3p14s$	21.1932	13.4132	0.0055	$3p14d$	21.1986	13.9236	0.0016
$3p15s$	21.2019	14.2593	0.0051	$3p15d$	21.2076	14.9102	0.0016

old. They used the noniterative eigenchannel *R*-matrix method and utilized a Hartree-Slater core potential to obtain wave functions. They showed that the mixing of the $2s\epsilon p$ and $2pns$ channels for the Be $^1P^o$ state can be described as an admixture of wave functions of these channels with almost equal amplitudes. As a result, the $2pns$ Rydberg series of doubly excited states interact very strongly with the $2s\epsilon p$ continuum, giving rise to broad autoionization resonances in the photoionization with excitation of Be from the ground state [5,6,13]. The narrow series is due to a much weaker interaction between the $2s\epsilon p$ and $2pnd$ channels, as also noted in the earlier calculations of Greene [5], O'Mahony and Greene [6], and Zhou and Lin [13]. Our calculation shows overall good agreement in shape and magnitude with their calculations. As noted above, there is excellent agreement between our length and velocity results, while the length and velocity values of O'Mahony and Greene [6] differ by about 20%. The HSCC calculation of Zhou and Lin [13] shows reasonable agreement between length and acceleration results except in the region of $2p3d$ and $2p4s$ resonances. It may be noted that the shape of the $2pnd$ resonance asymmetry features in their calculation does not agree with the shape in the present work or that of O'Mahony and Greene [6].

In Fig. 2(a) we display the present length form of the total photoionization cross section between the $Be^+(2p)$ and $Be^+(3s)$ thresholds as a function of photon energy. Again the OP results [9] are in good agreement with our calculation. The autoionizing Rydberg resonance series consists of the $3snp$ doubly excited states converging to the $Be^+(3s)$ threshold. However, there are three interlopers $3p3d$, $3p4s$, and $3d4p$ converging to $Be^+(3p)$ and $Be^+(3d)$ thresholds. To investigate these resonances in more detail, the region between 19.2 eV and the $Be^+(3s)$ threshold is shown in Fig. 2(b) as a function of photon energy. Table IV lists the present results of resonance positions, effective quantum numbers, and widths, along with the earlier experimental data [2,3]. Mehlman-Balloffet and Esteva [2] and Esteva *et al.* [3] did not assign the $3s5p$ resonance in their experi-

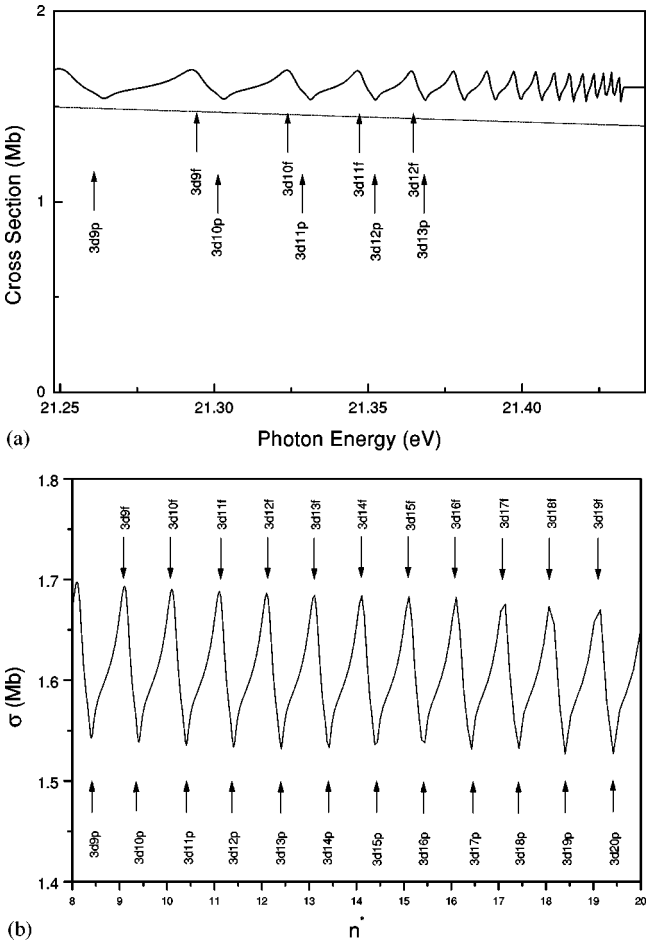

FIG. 5. Total photoionization cross section for the ground state of Be below the $Be^+(3d)$ threshold: (a) cross section as a function of photon energy in eV; (b) cross section as a function of effective quantum number n^*. Arrows indicate the positions of the autoionizing levels. Solid curve, present calculation; dotted curve, OP result [9].

TABLE VI. Resonance positions (E_r in eV), effective quantum numbers (n^*), and widths (Γ in eV) of autoionizing levels $3dnp$ and $3dnf$ converging to the $Be^+(3d)$ threshold.

State	E_r	n^*	Γ	State	E_r	n^*	Γ
$3d4p$	20.1120	3.1807	0.0053	$3d4f$	20.1980	3.2875	0.0062
$3d5p$	20.6070	4.0005	0.1856	$3d5f$	20.7268	4.3167	0.0063
$3d6p$	20.9317	5.0896	0.0171	$3d6f$	21.9877	5.3851	0.0054
$3d7p$	21.0988	6.1635	0.0114	$3d7f$	21.1311	6.4626	0.0040
$3d8p$	21.1924	7.1716	0.0024	$3d8f$	21.2188	7.5586	0.0042
$3d9p$	21.2639	8.3969	0.0160	$3d9f$	21.2950	9.1659	0.0052
$3d10p$	21.3028	9.3977	0.0113	$3d10f$	21.3252	10.1625	0.0048
$3d11p$	21.3312	10.4016	0.0082	$3d11f$	21.3475	11.1506	0.0045
$3d12p$	21.3524	11.4089	0.0062	$3d12f$	21.3649	12.1602	0.0041
$3d13p$	21.3684	12.4009	0.0048	$3d13f$	21.3782	13.1504	0.0037
$3d14p$	21.3812	13.4079	0.0038	$3d14f$	21.3888	14.1385	0.0034
$3d15p$	21.3913	14.3999	0.0031	$3d15f$	21.3975	15.1401	0.0031

ments. Bachau *et al.* [27] also calculated energies and widths of a few doubly excited states lying above the $Be^+(2p)$ threshold. However, they did not make assignments for these states, making it difficult to compare with our result. As shown in Fig. 2(b) and Table IV, there are significant series perturbations among the $3snp$ resonances. The two lowest resonances in this energy region are the $3s3p$ and $3s4p$ Rydberg states. Then the Rydberg state $3p3d$, which is the first member of the $3pnd$ series converging to the $Be^+(3p)$ threshold, is found at 19.391 eV just below the $3s5p$ state, showing a very narrow dip in the cross section. Another interloper, $3p4s$, which is the first member of the $3pns$ series converging to the $Be^+(3p)$ state, is found at 19.668 eV and it almost overlaps with the $3s5p$ state. As a result, there is an abnormal inflection point in the cross sections just above the $3s5p$ resonance. The perturbing state $3d4p$, the first member of the $3dnp$ series converging to the $Be^+(3d)$ threshold, is seen at 20.112 eV between the $3s11p$ and $3s12p$ states and it gives rise to a very narrow dip in the cross sections. The $3d4f$ state is not seen in Fig. 2(b) because it lies just below the $Be^+(3s)$ threshold. Owing to these perturbations, the quantum defects along the $3snp$ series converging to the $Be^+(3s)$ threshold do not approach an asymptotic quantum defect even at $n=15$, as seen in Table IV.

Since there are three open channels $2s\epsilon p$, $2p\epsilon s$, and $2p\epsilon d$ in this energy range, partial photoionization cross sections related to these three channels are shown in Figs. 3(a), 3(b), and 3(c) in both length and velocity gauges. The length results are shown by solid curves and the dashed curves show the velocity values. Our cross sections in this region can be compared with those of Zhou and Lin [13]. As well as we can read the data from the figures of [13], there appears to be very good overall agreement between the two calculations in each of the channels. The background cross sections in the $2s\epsilon p$ channel are much larger than for the other two channels, as also noted by Zhou and Lin [13]. This is expected since the $2s\epsilon p$ is the single-electron ionization channel; the other two channels represent ionization plus excitation.

The present total photoionization cross section between the $Be^+(3s)$ and $Be^+(3p)$ thresholds is given in Fig. 4(a) along with that of the OP [9]. The arrows indicate the assignments of the lower autoionizing Rydberg resonances shown

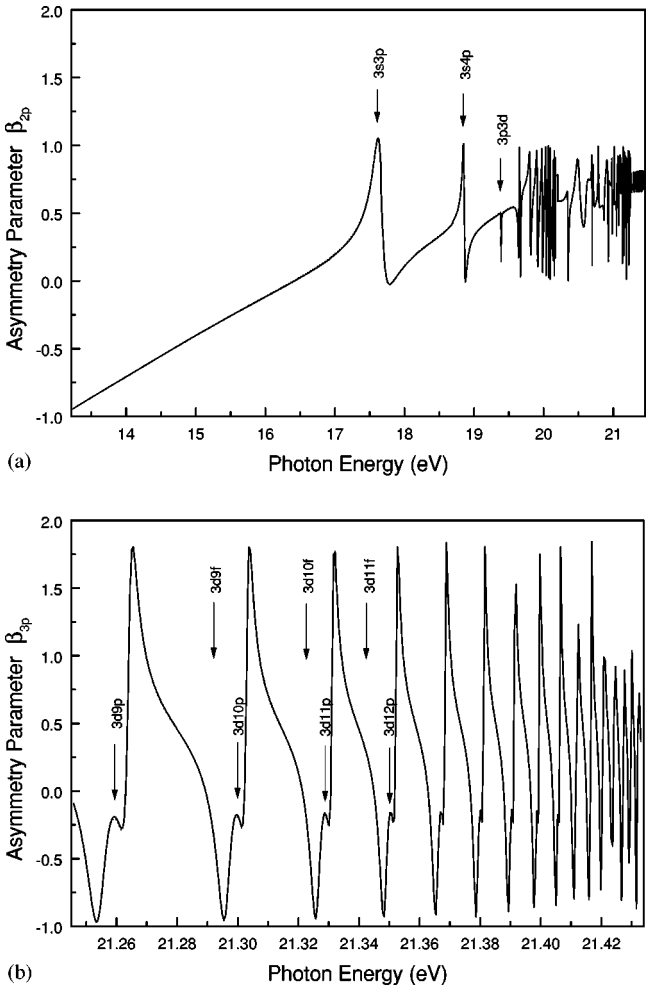

FIG. 6. Photoelectron angular distribution asymmetry parameter β as a function of photon energy in eV: (a) β_{2p}; (b) β_{3p}.

in our solid curve. There is reasonable agreement between the two calculations except that the OP results are shifted to a lower energy by about 0.055 eV. The resonances above the $3p9s$ autoionizing level are shown in Fig. 4(b) as a function of effective quantum number n^*. There are four open channels $2s\epsilon p$, $2p\epsilon s$, $2p\epsilon d$, and $3s\epsilon p$ in this energy region. The Rydberg series in this energy range are $3pns$ and $3pnd$ converging to the $Be^+(3p)$ threshold. Lower members of the Rydberg series $3dnp$ and $3dnf$ $(n<9)$ converging to the $Be^+(3d)$ threshold also lie in this energy region because the energy difference between the $Be^+(3p)$ and $Be^+(3d)$ thresholds is only 0.188 eV. These resonances are quite complex. However, many of these resonances have been identified using the technique of eigenphase gradients as discussed earlier, and the resonance parameters are listed in Table V. The total photoionization cross sections above the $Be^+(3p)$ threshold up to $Be^+(3d)$ are shown in Fig. 5(a) vs energy and Fig. 5(b) vs effective quantum number. As shown in Fig. 5(a), the OP results [9] do not include the autoionizing resonances due to the doubly excited states $3dnp$ and $3dnf$ in this region; however, their background cross section is accurate. The resonance parameters in this energy region are tabulated in Table VI.

The behavior of the angular distribution asymmetry parameters β_{2p} and β_{3p} leaving the ion in the $Be^+(2p)$ and $Be^+(3p)$ excited states has not been investigated previously to our knowledge. Our results for β_{2p} and β_{3p} are shown in Figs. 6(a) and 6(b), respectively. The angular distribution asymmetry parameter β_{2p} at the $Be^+(2p\ ^2P)$ threshold is almost -1 and it increases monotonically with increasing energy with peaks around the resonances. In order to explain this behavior, we need to investigate the expression for β_{np} given in Eq. (2.22), which can be broken up as

$$\beta_{np}=\tau_1+\tau_2, \quad n=2,3, \tag{3.5}$$

where

$$\tau_1=\frac{d_{\epsilon d}^2}{d_{\epsilon s}^2+d_{\epsilon d}^2}, \tag{3.6}$$

$$\tau_2=\frac{2\sqrt{2}\ \mathrm{Re}(d_{\epsilon s}d_{\epsilon d})\cos\sigma}{d_{\epsilon s}^2+d_{\epsilon d}^2}. \tag{3.7}$$

The $\cos\sigma$ term is nearly -1 at the $Be^+(2p)$ threshold, and increases slowly with increasing energy to about zero at the $Be^+(3s)$ threshold. Thus, $\cos\sigma$ is negative in this energy region, and the term τ_2 is also negative. At threshold, the term τ_2 is dominant since $\cos\sigma\approx-1$, then increases with increasing energy. At 16.430 eV, τ_1 and τ_2 have the same magnitude with opposite sign; as a result β_{2p} is zero at this energy. Above this energy, τ_1 dominates, so that β_{2p} becomes positive at this point. With increasing energy, $\cos\sigma$ becomes more and more positive, leading to a gradual increase of the background β_{2p}. However, the various resonances dominate β_{2p} over the entire higher energy range. The β_{3p} for the $Be^+(3p\ ^3P)$ channel, shown in Fig. 6(a), is entirely dominated by the $3dnp$ and $3dnf$ resonances. It is interesting to note that the resonances are much more well defined in β as opposed to cross sections [cf. Fig. 5(a)]. This speaks to the importance of measurements of β, as well as cross sections, to better understand the photoionization dynamics of atomic and ionic systems.

IV. CONCLUSIONS

Total and partial photoionization cross sections for the ground $1s^22s^2\ ^1S$ state of atomic beryllium in the energy range from the $Be^+(2s)$ to the $Be^+(3d)$ threshold are presented. The photoionization cross section is dominated by Rydberg series of autoionizing resonances converging to various ionic thresholds. A detailed analysis and identification of these autoionizing levels is presented; a process made difficult by the overlap of the various series converging to different thresholds. However, using the ideas of eigenphase sum gradients [25], major resonances have been identified. The photoelectron angular distribution asymmetry parameters β_{2p} and β_{3p} for ionization to $Be^+(2p)$ and $Be^+(3p)$ are reported. The present results extend and improve upon earlier calculations. It is hoped that the accurate calculations presented will stimulate future experiment to corroborate our claim of accuracy.

This work will be extended in several directions: First, to the photoionization of the excited $1s^22s2p\ ^{1,3}P$ states of Be; the ^3P state is metastable, which is of importance astrophysically. In addition, the photoionization of the Be isoelectronic sequence will be considered, ground and excited states, both to understand the evolution of the resonances and to provide accurate data on these systems for astrophysical data bases.

ACKNOWLEDGMENTS

Discussions with F. Robicheaux are gratefully acknowledged. This research work was supported by the National Science Foundation under Grant No. AST-9528945 and by NASA.

[1] P. L. Altick, Phys. Rev. **169**, 21 (1968).
[2] G. Mehlman-Balloffet and J. M. Esteva, Astrophys. J. **157**, 945 (1969).
[3] J. M. Esteva, G. Mehlman-Balloffet, and J. Romand, J. Quant. Spectrosc. Radiat. Transf. **12**, 1291 (1972).
[4] J. Dubau and J. Wells, J. Phys. B **6**, L31 (1973).
[5] C. H. Greene, Phys. Rev. A **23**, 661 (1981).
[6] P. F. O'Mahony and C. H. Greene, Phys. Rev. A **31**, 250 (1985).
[7] V. Radojevic and W. R. Johnson, Phys. Rev. A **31**, 2991 (1985).
[8] R. Moccia and P. Spizzo, J. Phys. B **16**, 723 (1985).
[9] J. A. Tully, M. J. Seaton, and K. A. Berrington, J. Phys. B **23**, 3811 (1990).

[10] K. A. Berrington, P. G. Burke, M. J. Seaton, P. J. Storey, K. T. Taylor, and Yan Yu, J. Phys. B **20**, 6379 (1987).
[11] H.-C. Chi, K.-N. Huang, and K. T. Cheng, Phys. Rev. A **43**, 2542 (1991).
[12] T. N. Chang and X. Tang, Phys. Rev. A **44**, 232 (1991); **46**, R2209 (1992); T. N. Chang and L. Zhu, *ibid.* **48**, R1725 (1993).
[13] B. Zhou and C. D. Lin, Phys. Rev. A **51**, 1286 (1995).
[14] F. Robicheaux, Phys. Rev. A **43**, 5946 (1991).
[15] F. Robicheaux and C. H. Greene, Phys. Rev. A **46**, 3821 (1992); **47**, 1066 (1993); **48**, 4441 (1993).
[16] W. R. Johnson, D. Kolb, and K.-N. Huang, At. Data Nucl. Data Tables **28**, 333 (1983).
[17] U. Fano and A. R. P. Rau, *Atomic Collisions and Spectra* (Academic, Orlando, FL, 1986).
[18] C. H. Greene and Ch. Jungen, Adv. At. Mol. Phys. **21**, 51 (1985).
[19] C. N. Yang, Phys. Rev. **74**, 764 (1948).
[20] M. Aymar, C. H. Greene, and E. Luc-Koenig, Rev. Mod. Phys. **68**, 1015 (1996).
[21] S. T. Manson and A. F. Starace, Rev. Mod. Phys. **54**, 389 (1982).
[22] U. Fano and D. Dill, Phys. Rev. A **6**, 185 (1972).
[23] S. T. Manson, J. Electron Spectrosc. Relat. Phenom. **1**, 413 (1973).
[24] C. E. Moore, Atomic Energy Levels, Natl. Bur. Stand. (U.S.) Circ. No. 467 (U.S. GPO, Washington, DC, 1949), Vol. I.
[25] L. Quigley and K. Berrington, J. Phys. B **29**, 4529 (1996). See also L. Quigley, K. Berrington, and J. Pelan, Comput. Phys. Commun. **114**, 225 (1998); C. P. Ballance, K. A. Berrington, and B. M. McLaughlin, Phys. Rev. A **60**, R4217 (1999).
[26] E. Luc-Koenig, M. Aymar, and J. M. Lecomte, J. Phys. B **27**, 2447 (1994).
[27] H. Bachau, P. Galan, F. Martin, A. Riera, and M. Yanez, At. Data Nucl. Data Tables **44**, 305 (1990).